QUANTIFYING THE MICROMECHANICAL EFFECTS OF VARIABLE CEMENT IN GRANULAR POROUS MEDIA

PI: Laurel B. Goodwin; Ph.D. Student: Jennie E. Cook; University of Wisconsin - Madison
PI: David F. Boutt; M.S. student Katherine Plourde; University of Massachusetts, Amherst

DOE Award Number FG02-05ER15738
Award Period: 8/15/05-8/14/09; Date of Report: 2/18/2010

Abstract

The mechanical and hydrologic behavior of clastic rocks and sediments is fundamentally controlled by variables such as grain size and shape, sorting, grain and cement mineralogy, porosity, and %cement - parameters that are not used directly in field-scale models of coupled flow and deformation. To improve our understanding of the relationship between these micromechanical properties and bulk behavior we focused on (1) relating detailed, quantitative characterization of the grain-pore systems to both hydrologic and mechanical properties of a suite of variably quartz-cemented quartz arenite samples and (2) the use of a combination of discrete element method (DEM) and poroelastic models parameterized by data from the natural samples to isolate and compare the influence of changes in the mechanical and hydrologic properties of granular porous media due to changes in degree of cementation.

Quartz overgrowths, the most common form of authigenic cements in sandstones, are responsible for significant porosity and permeability reduction. The distribution of quartz overgrowths is controlled by available pore space and the crystallographic orientations of individual quartz grains. Study of the St. Peter Sandstone allowed evaluation of the relative effects of quartz cementation and compaction on final grain and pore morphology, showing that progressive quartz cementation modifies the grain framework in consistent, predictable ways. Detailed microstructural characterization and multiple regression analyses show that with progressive diagenesis, the number and length of grain contacts increases as the number of pores increases, the number of large, well-connected pores decreases, and pores become rounder. These changes cause a decrease in pore size variability that leads to a decrease in bulk permeability and both stiffening and strengthening of the grain framework.

The consistent nature of these changes allows us to predict variations in hydrologic and mechanical properties with progressive diagenesis, and explore the impact of these changes on aquifer behavior. Several examples of this predictive capability are offered. In one application, data from natural sandstones are used to calibrate the proportionality constant of the Kozeny-Carman relationship, improving the ability to predict permeability in quartz-cemented quartz arenites. In another, the bond-to-grain ratio (BGR) is used to parameterize a discrete element model with data acquired from sandstone samples. The DEM results provide input to poroelastic models used to explore the hydrologic, mechanical, and coupled hydrologic and mechanical response of the sandstone to pumping stresses. This modeling exercise shows that at the macro-scale, changes in mechanical and hydrologic properties directly influence the magnitude and area of aquifer deformation. The significant difference in sensitivity of the system to the mechanical properties alone versus its sensitivity to coupled mechanical and hydrologic properties demonstrates the importance of including hydrologic properties that are adjusted for changes in cementation in fluid storage and deformation studies. The large magnitude of radial deformation

compared to vertical deformation in these models emphasizes the importance of considering three dimensional deformation in fluid flow and deformation studies.

Introduction

Diagenesis changes the geometry and morphology of the grain framework and pore network of a clastic sedimentary rock. These changes impact the mechanical and hydrologic behavior of the resulting lithified material. The primary focus of our DOE-funded research has been to quantify these diagenetic changes and their effects on mechanical and hydrologic properties in natural sandstones, then use the results of these studies to improve numerical models to explore the poroelastic response of fluid-sandstone systems to pumping and injection. Because variables such as mineralogy, grain size, grain shape, and sorting may influence these effects, we have deliberately chosen a simple system for the heart of our work (though we also have conducted exploratory studies of more complex systems). The Ordovician St. Peter Sandstone, the focus of our research effort, is a remarkably pure, well sorted quartz arenite, with unusually well rounded grains (Odom et al., 1979; Mai and Dott, 1985). In south-central Wisconsin where we sampled the sandstone, only magnitude of compaction and percent cement exhibit significant variability. The cement, like the grains, is quartz, allowing us to consider the physical effects of geometric and morphologic changes associated with cementation without the complicating effect of contrasting material properties of grains and cement.

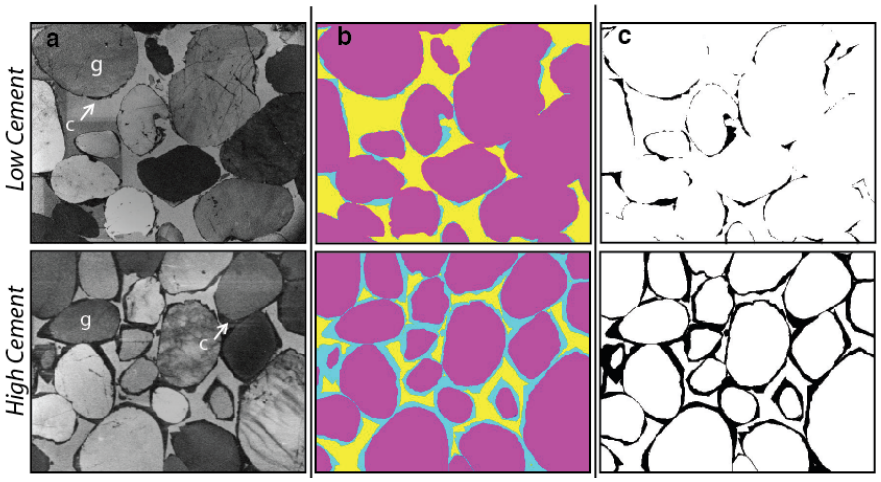

Figure 1 - Comparison of cement micromorphology with low (3.5%) and relatively high (15.6%) cement abundance. (a) CL images in which grains *(g)* are distinguished from cement *(c)* by differences in luminescence. (b) False-color images of the same areas. Cement is blue, grains are magenta, and pores are yellow. The intergranular area of the two images is roughly the same, but porosity in the high cement example is less than half that of the low cement example. (c) Images showing only areas of cement.

Theoretical models represent the process of cementation as a simple one, with cement added systematically and uniformly at grain contacts and/or as concentric growth rings around grains (Dvorkin and Yin, 1995; Wong and Wu, 1995; Dillon et al., 2004) or as pore fill (Panda and Lake, 1995). Natural sandstones, however exhibit grain- and pore-scale geometries that demonstrate that grain and cement mineralogy control the cementation process and therefore resulting geometries. For example, although calcite cement is uniformly distributed in carbonate sediments, it is typically poikilotopic in quartz arenites, such that large calcite crystals locally engulf detrital quartz grains and fill porosity, but intervening sediment remains uncemented (Scholle, 1979). Quartz cement, in contrast, is typically precipitated as overgrowths on quartz grains with a geometry that is crystallographically controlled, and is relatively uniformly

distributed in quartz arenites. These differences in geometry and spatial distribution will have mechanical and hydrologic impacts beyond those produced by the differing mechanical properties of the cementing material. The system we chose to study is arguably one most similar to the conceptual model described by Dvorkin and Yin (1995); others are expected to exhibit different hydrologic and mechanical behavior with progressive diagenesis.

The syntaxial quartz overgrowths exhibited by the St. Peter Sandstone are the most common form of authigenic cement in quartz sandstones (McBride, 1989; Worden and Morad, 2000). At early stages of quartz cementation, quartz cement largely precipitates at narrow constrictions, particularly at grain contacts, but late-stage cement growth is crystallographically and space controlled (McBride, 1989). Examples of variably cemented quartz arenite samples from the St. Peter Sandstone are shown in **Figure 1**. Grains in low-cement (< 5%) samples exhibit thin, encrusting layers of quartz with isolated crystal facets and interconnected pore spaces. In contrast, high-cement (> 10%) samples have an interconnected network of cement with well-defined facets and diminished pore connectivity. We have quantified these changes in the solid framework and pore network, focusing on parameters likely to influence material properties of interest. For example, pore shape demonstrably influences both compressibility and the response of the system to changing pore pressure (e.g., Storvoll and Bjorlykke, 2004), so we have documented the evolution of pore shape with progressive diagenesis. In addition, we explicitly considered the effect of compaction, often the greatest cause of porosity reduction (Lundergard, 1991). Statistical analyses provide an objective approach to evaluating the relative effects of compaction and cementation on hydrologic and mechanical characteristics. This work demonstrates systematic – and therefore predictable – changes in rock properties with

Table 1 - Sample characteristics, listed from highest to lowest porosity. CC - clay coatings; P - pyrite; IC - iron oxide cement.

Sample	Mean Porosity (%) (Image Analysis)	Porosity (%) (Pycnometer)	Mean Quartz Cement (%)	K-Spar Cement (%)	Mean IGV (%)	Avg. Grain Size (mm)	Other Phases
1_2	24.6		5.9	0.2	30.9	0.20	
5_2	24.4	25.3	0.9	0.9	26.4	0.17	IC
13_1	20.7	21.0	9.4	0.0	30.2	0.19	P, CC
14_1	19.5		0.6	0.7	20.9	0.17	IC
4_1	19.0		8.1	0.6	28.0	0.20	
3_2	16.6	14.9	11.5	0.6	28.7	0.17	IC
3_1	15.3	15.3	13.4	0.5	28.9	0.15	IC
11_2	12.4	12.4	11.4	1.0	24.3	0.15	IC
12_1	8.7	8.1	16.6	0.1	25.3	0.17	IC, CC

progressive diagenesis.

Our work has been a collaborative effort between the University of Massachusetts - Amherst (UMass, PI David Boutt), the University of Wisconsin - Madison (UW, PI Laurel Goodwin), and Sandia National Labs (PIs Thomas Buchheit and Benjamin Cook). This report focuses on the university effort. In the following sections, we summarize the results of the UW-led investigation into the evolution of the grain-pore system of quartz-cemented quartz arenites

with progressive diagenesis, and its impact on permeability (Cook et al., in review). Subsequently, we explore relationships between the grain, cement, and pore parameters identified in the latter study and relate them to both elastic and inelastic mechanical properties (Cook et al., in prep.). To demonstrate how these data can be used in predictive models, we show key results of a UMass-led exploration of the relative importance of hydrologic and mechanical constraints on poroelastic models (Plourde et al., in prep.). A final section briefly outlines results of other projects that were supported in part by DOE funds.

UW Study of Natural Sandstone: Summary of Cook et al. (in review)

Sample Characterization

As indicated above, our work has focused on the St. Peter Sandstone. Burial in Wisconsin, where we sampled the sandstone, is constrained to less than 1000m (Kelly et al., 2007). In samples selected for this study, quartz is the only primary grain type present. Grains consist of fine- to medium-sized, very well sorted and well rounded sand. Quartz overgrowths are the dominant form of cement; minor diagenetic phases including pyrite and iron oxide cements, potassium feldspar overgrowths, and clay coatings are only locally evident. Nine samples exhibiting a wide range in porosity and % quartz cement were selected for detailed study. Six of these are mesoscopically homogeneous, with no evidence of bedding at the sample scale, and three samples contain cm-scale bedding.

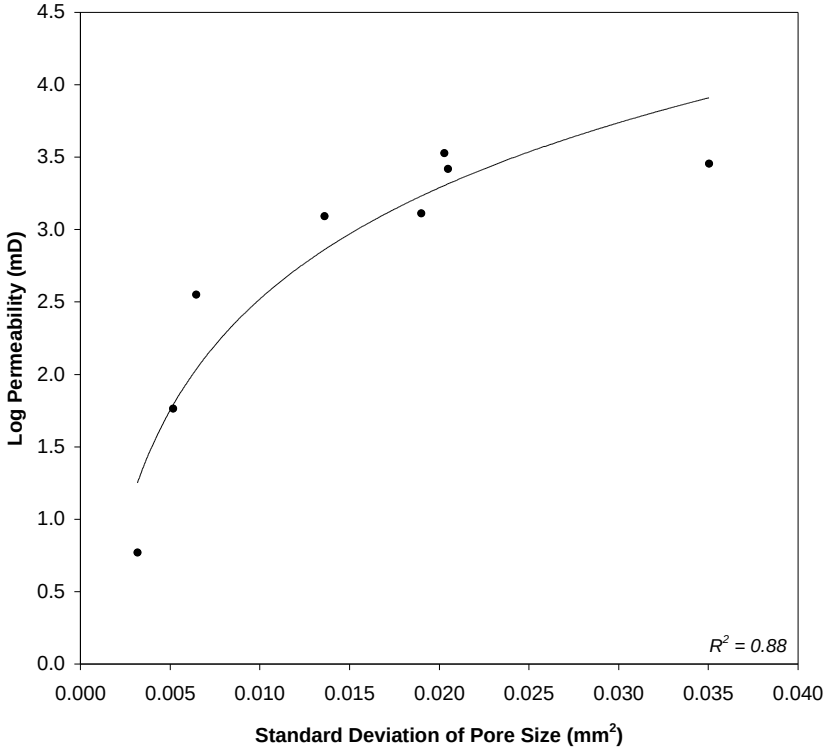

Figure 2 – Plot of log permeability versus pore size variation, showing the effects of progressive diagenesis.

Progressive diagenesis changes both connectivity in the solid framework and pore size and shape – changes we refer to in terms of micromorphology. Quantification of the micromorphology of variably cemented St. Peter Sandstone samples allows investigation of the relationships between these features and properties of interest, such as permeability and compressive strength. To evaluate micromorphology, a series of backscattered electron (BSE), cathodoluminescent (CL; **Figure 1**), and secondary electron (SE) image mosaics were constructed for each sample. Mosaics represent areas of the samples that range in size from

approximately 4.4 mm by 3.3 mm to 3.7 mm by 2.7 mm and consist of 36 or 25 images collected at 150x magnification, respectively.

In addition to more typically acquired variables such as grain size, modal mineralogy, cement, and porosity (**Table 1**), we measured (1) grain-contact parameters: bond-to-grain ratio (BGR) and the mean length of contacts between touching grains; and (2) pore parameters: pore area, number of pores, pore circularity, pore size variability, and specific surface area. The latter is one of the variables used to estimate permeability using the Kozeny-Carman relationship (Panda and Lake, 1994; Mowers and Budd, 1996).

The data collected show consistent trends. Both BGR and pore number increase as porosity decreases, cement content increases, and inter-granular volume (IGV=%cement + %porosity) decreases with progressive diagenesis. Both mean pore size and variation in mean pore size decrease, however, as the rock becomes better cemented. Average contact length increases with both grain size and percentage cement. Pores generally become more circular with increasing cementation and decreasing IGV, as shown by shape factors that approach 1.

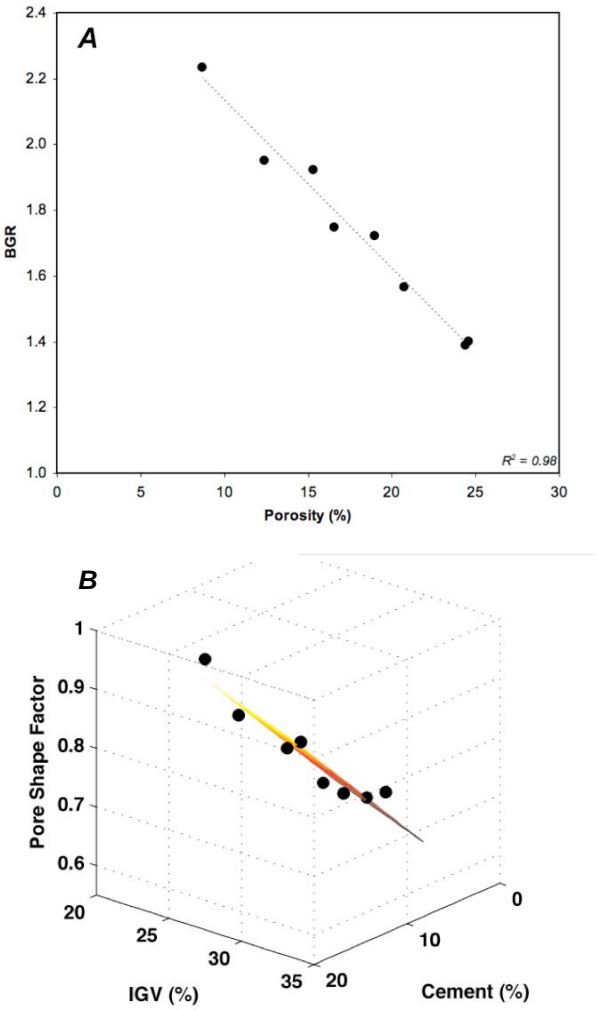

Figure 3 – Graphical results of example multiple regression analyses. (A) BGR is strongly correlated to porosity, regardless of the means of porosity reduction. (B) Pore shape is determined by IGV and cement percentage, and is therefore path-dependent.

Diagenesis and Permeability

Permeability measurements were conducted by New England Research at a confining pressure of 14.5 MPa, representing the maximum 1 km burial depth and hydrostatic fluid pressure inferred for St. Peter Sandstone in the study area. Samples with expected permeabilities greater than 500 mD were analyzed using a steady-state flow technique; a transient pressure technique was used to determine the permeability of low-porosity samples. Both methods were used to determine the permeability of an intermediate porosity sample, showing results of the same order of magnitude. As expected, permeability decreases with porosity as cement percentage increases; destruction of the largest pores with progressive cementation results in an exponential decrease in both permeability and pore size variation (**Figure 2**).

Statistical analysis

To investigate the relative impacts of diagenetic path on sample characteristics, data were analyzed using stepwise multiple regression. For each dependent parameter, we considered two primary models: (1) regression with respect to porosity; and (2) regression with respect to IGV and % quartz cement. The first of these models will result in the best fit for variables that are not sensitive to diagenetic path, but respond only to changes in porosity, regardless of how those are effected. The second model indicates that path is important; that is, reduction in IGV through compaction and reduction in porosity through cementation leave independent 'signatures' in the resulting micromorphology. Mean grain size was an additional predictor variable considered for each model.

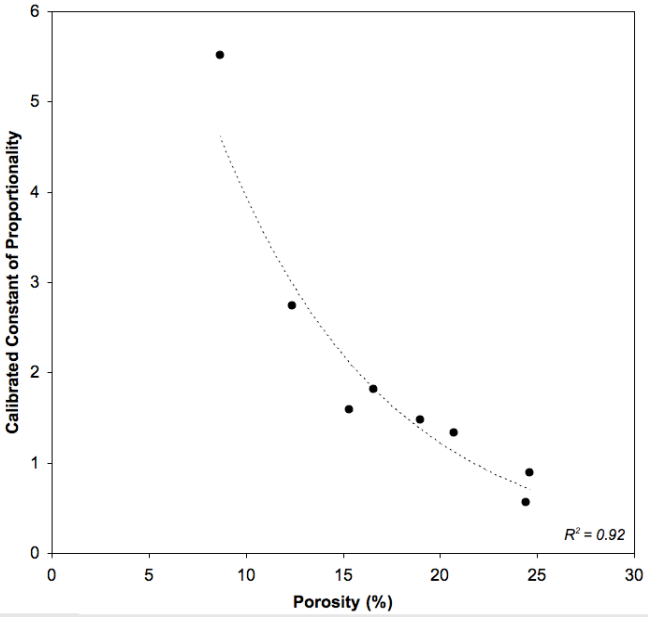

Figure 4 – Plot showing exponential increase in proportionality constant with decreasing porosity. Note the order of magnitude difference in values for the range in porosity considered.

Regression results indicate that BGR, specific surface area, and pore size variability can be approximated as a function of porosity loss alone, thus the method of pore occlusion is unimportant. For example, BGR changes by approximately 0.26 for each 5% change in porosity (**Fig. 3a**). Specific surface area has the most unexplained variability in the data. Average pore size and number of pores are best approximated as a function of both porosity and grain size. Thus, the method of porosity reduction is unimportant for these parameters as well, but grain size matters.

Two parameters were found to be sensitive to diagenetic path: grain contact length and pore shape (**Fig. 3b**). Pore shape is a function of IGV and cement %, whereas average grain contact length is a function of IGV, % cement, and grain size. Cementation results in more circular pores than physical compaction alone. The magnitude of regression coefficients suggest that cementation is at least twice as important as changes in IGV to resulting contact length.

An Approach to Improving Permeability Estimates

When permeability measurements are not available, the permeability of a granular porous medium of interest is often estimated using an empirical or theoretical model such as the widely used Kozeny-Carman relationship. The latter relates two parameters that are easily acquired from an image of a grain-pore network - specific surface area and porosity (Panda and Lake, 1994; Mowers and Budd, 1996) - to permeability as follows:

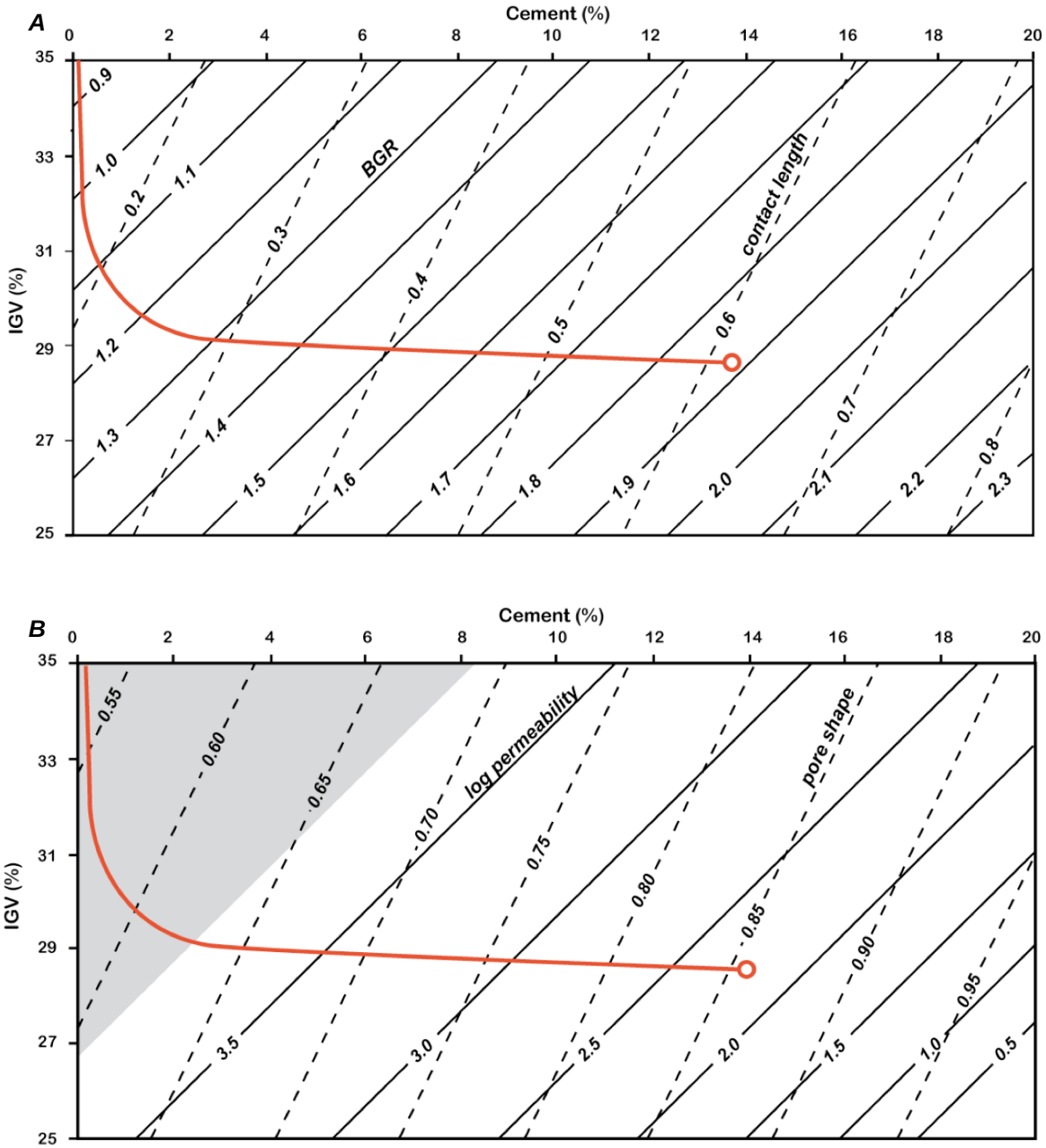

Figure 5 – Schematic diagrams show changes in key variables with progressive diagenesis (involving reduction in IGV through compaction as well as further changes in the grain-pore system with increasing cement content). Contours of these variable values, shown as dashed and solid lines, are based on regression analyses. The red line in both figures illustrates the interpreted grain-pore evolution with diagenesis of sample 3_1. For cases where the value of the dependent parameter is a function of porosity, the value changes equally for a reduction in IGV or equal increase in % cement (porosity = IGV - % cement). (A) BGR (solid lines) and contact length in mm (dashed lines) predicted for sandstones with a mean grain size of 0.15 mm. Plot can be adapted for other grain sizes by adding 0.023 mm to the contour values for contact length for each 0.05 mm increase in grain size. (B) Log permeability in mD (solid lines) and pore shape (dashed lines) predicted for a variety of IGV and cement percentages. Area shown in gray is outside of the calibration data set for permeability, thus no predictions are made.

$$k = \frac{\phi^3}{K_0(\frac{L_0}{L_E})^2(1-\phi)^2 SSA^2},$$

where k is permeability, φ is porosity, K_0 is an empirical Kozeny constant related to the cross-sectional area of the pore, L_0/L_E is the tortuosity, and SSA is the specific surface area. A proportionality constant, ***c***, is typically substituted for the $K_0(L_0/L_e)$ parameter (Mowers and Budd, 1996). A value of 5 is commonly assigned to ***c***, but this constant of proportionality should vary with the pore system (Carman, 1956; Mowers and Budd, 1996).

As our data illustrate, diagenesis alters the amount and distribution of pore space, creating smaller, more disconnected pores. We therefore used our data to test the hypothesis that a uniform constant of proportionality is not sufficient to describe the differences in permeability related to physical compaction and cementation. To do this, we calculated a raw, uncorrected permeability (***k***) from the Kozeny-Carman relationship without the proportionality constant,

$$k = \frac{\phi^3}{(1-\phi)^2 SSA^2},$$

and then determined the value of ***c*** needed to make the calculated permeability equivalent to the permeability predicted using the equation from our regression analysis. We used values of permeability from the regression analysis rather than the individual measured values to minimize the effect of natural sample variability. These calculations indicate that for accurate predictions of permeability within this dataset, the constant of proportionality for the pore systems decreases exponentially with increasing porosity (i.e. decreasing diagenetic alteration) (**Figure 4**). These data demonstrate that the commonly utilized value of 5 is not appropriate for this sample set. In total, the calculated constants span an order of magnitude, and most values are less than 2.

Diagenesis/Permeability Pathways

During progressive burial and diagenesis of quartz arenites large pores are progressively destroyed, causing the number of small pores to increase, pore size to become more homogeneous, and pore connectivity to decline. Accompanying these changes are increasing number and length of grain contacts. Compaction increases grain contacts because pore spaces collapse and are reorganized, whereas cementation increases bridges between grains. If grains were perfectly spherical, compaction alone would not increase grain contact length. However, because they are irregularly shaped, increased compaction will result in more efficient grain packing, increasing contact length. The addition of cement lengthens grain contacts, and the preferential precipitation of cements at narrow grain contacts amplifies this effect.

Average pore size decreases as expected with porosity; however, this reduction is achieved primarily through destruction of the largest pores, producing multiple smaller pores. These largest, well-connected pores primarily control permeability. As they are preferentially destroyed, permeability and pore size variation decrease exponentially. Specific surface area also decreases with decreasing porosity and destruction of the largest pores. The data collected, and regression analyses showing relationships between these data, can be used to predict changes in parameters

of interest with progressive diagenesis in quartz-cemented quartz arenites. To illustrate this point, we show how the physical properties BGR, mean contact length, pore shape, and permeability vary with compaction (which reduces IGV) and cementation (which reduces porosity; **Figure 5**). The inferred history of our sample 3_1 (shown as red lines in **Figure** 5**)** demonstrates the importance of burial path for some parameters. A sample that experienced less compaction prior to cementation, for example, would retain a higher permeability at any given cement percentage.

The number of pores does not stay the same with continued diagenesis (Gal et al., 1998). Our data show that the number of pores increases, regardless of whether porosity reduction is dominated by compaction or cementation. In addition, pore size decreases and becomes more homogeneous, and pores become progressively more spherical with increasing diagenesis. These changes have implications for mechanical, as well as hydrologic properties.

UW Study of Natural Sandstone: Summary of Cook et al. (in prep)

Mechanical effects of diagenesis

Understanding and developing predictive models relating the mechanical behavior of rocks to progressive diagenesis is of interest for a number of geologic and engineering applications, all of which have implications for subsurface CO_2 sequestration. For example, it is desirable to predict mechanical behavior from in-situ tests because rock strength influences well bore stability, sanding, and hydrofracture potential. Diagenetic controls on both the style and

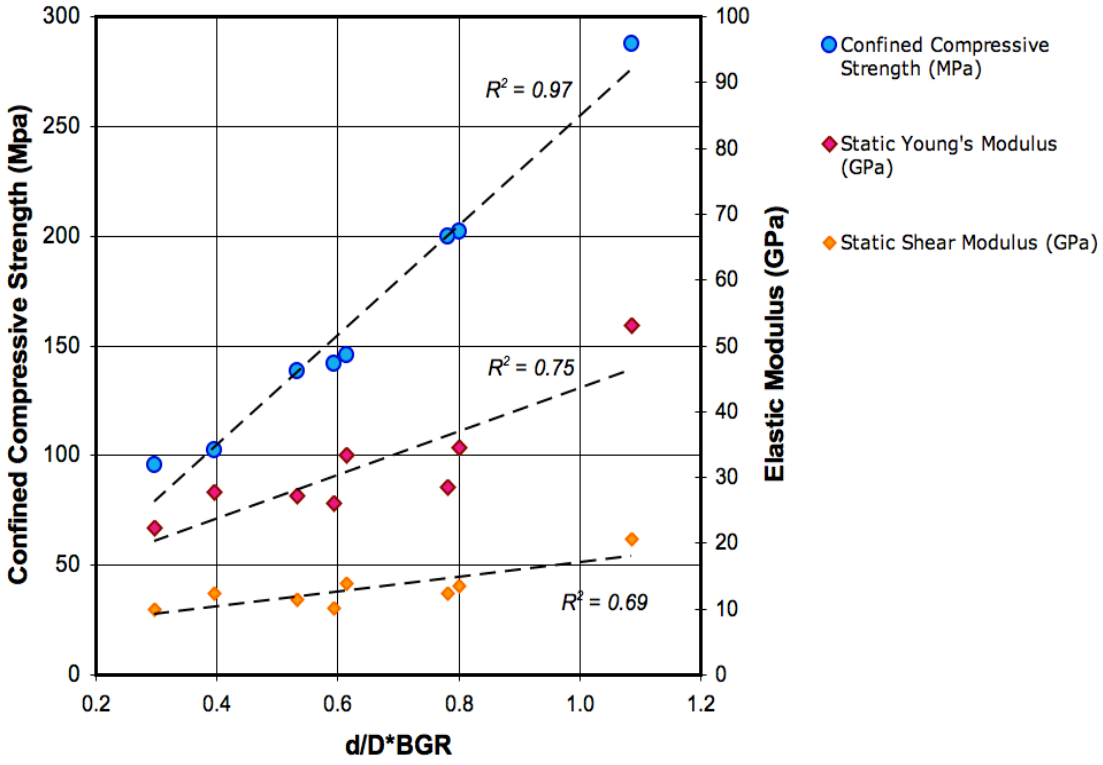

Figure 6 – Confined compressive strength and static moduli increase linearly with d/D*BGR.

distribution of structural features such as deformation bands, faults, and fractures are important

because these different structures affect fluid flow in very different ways. For example, Dunn et al. (1973) identified an important transition in deformation behavior in sandstones that corresponded with ~12% porosity. In their experimental study, sandstones with porosities greater than this threshold failed through the formation of deformation bands, whereas sandstones with lower porosities failed through the formation of through-going fractures.

The importance of porosity in influencing mechanical behavior is recognized by mechanical models fundamentally based on percent porosity, which is fortunately a relatively easy parameter to estimate from borehole geophysical tests. However, both the amount and the *distribution* of porosity are primary controls on mechanical behavior.

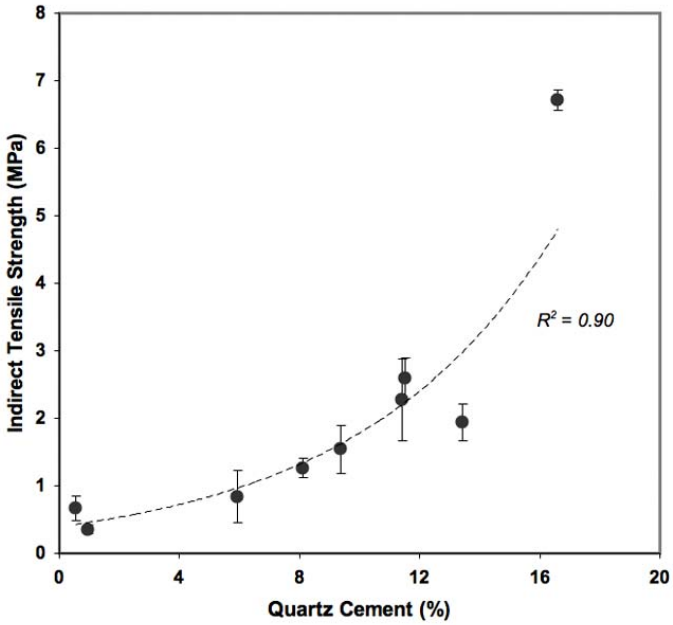

Figure 7. Tensile strength increases exponentially with quartz cement within the range of porosity tested (~8-25%). Error bars show 2 sigma variation in results of three tests per sample.

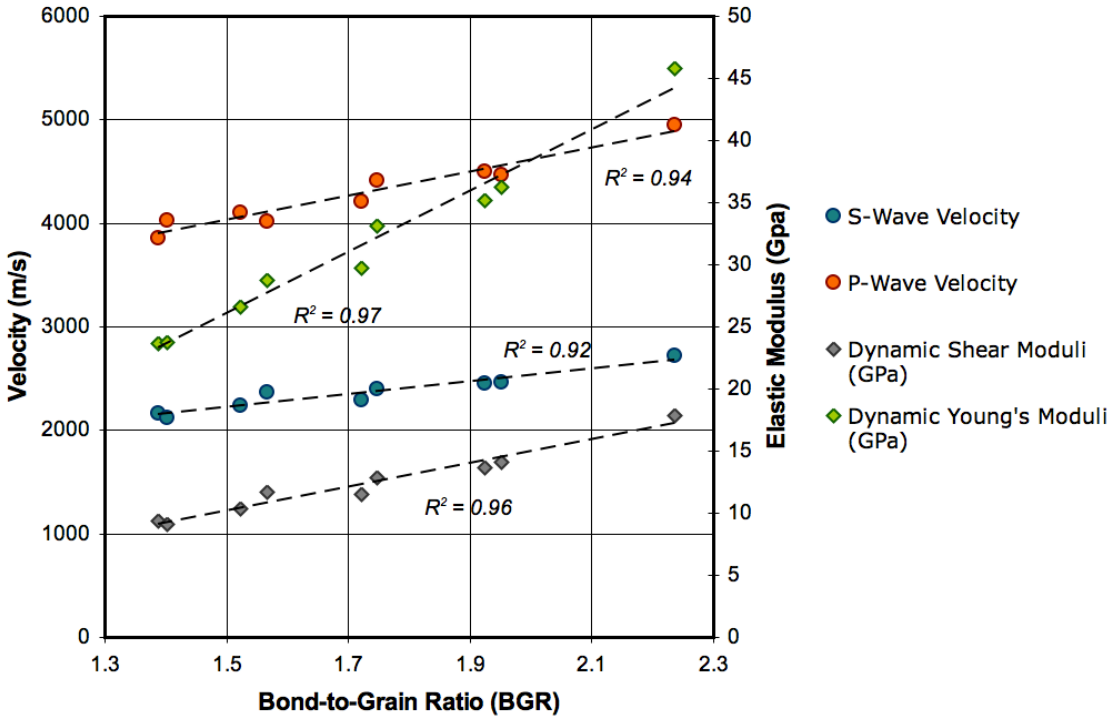

Figure 8 – Dynamic mechanical properties of the St. Peter Sandstone plotted with respect to bond-to-grain ratio.

Because the geometric arrangement of pores and grains is rarely known, effective media theories including Voigt and Reuss (Reuss, 1929) and Hashin-Shtrikman (Hashin and Shtrikman, 1963) are used to predict upper and lower bounds for elastic moduli based on the elastic moduli of the constituent phases and the volume fractions occupied by those constituents (see summary of approaches in Mavko et al., 2003). These can be useful approximations; however, the precision of a given prediction is limited by knowledge of the amounts and distribution of the rock constituents. Our research is therefore based on the premise that considering the geometry of cement precipitation could lead to more general models of mechanical behavior.

Compaction, cementation, and pressure solution affect a sandstone volume differently. Physical and chemical compaction are volume *reducing* processes, whereas cementation *preserves* net volume. Through physical compaction, the grain framework is reorganized but preserved but porosity is both reduced and redistributed. By chemical compaction, grain material is removed, resulting in simultaneous pore-size and porosity reduction. And cementation adds material to the grain framework with associated reduction in pore space. Thus, compaction and cementation affect both the amount and the way that porosity is distributed in different ways. Developing a quantitative understanding of how diagenetic path affects the distribution of porosity will allow for better prediction of mechanical behavior.

Mechanical Tests

To investigate the mechanical effects of the micromorphologic changes we have documented in samples of St. Peter Sandstone, static elastic moduli and compressive strength tests of the same samples were conducted by New England Research at a confining pressure of 14.5 MPa, representing the maximum 1 km burial depth and hydrostatic fluid pressure inferred for the sandstone in the study area. Brazilian tests conducted at UW-Madison provide estimates of unconfined tensile strength. We also measured ultrasonic velocities and calculated dynamic elastic properties. The latter data provide not only additional information about the mechanical behavior of these samples, but also a mechanism for linking laboratory study with subsurface analysis through borehole geophysics.

The results of these analyses are summarized in **Figures 6-8**. In each case, test results are plotted with respect to the micromorphologic parameter that best fits the data. In addition to variables discussed previously, we considered the effect of contact strength using the parameter d/D*BGR, where (d) is the average contact length and (D) is the average grain diameter. Confined compressive strength data show an extraordinarily good linear fit to d/D*BGR; more variable static elastic moduli are less well fit by d/D*BGR (**Figure 6**). Tensile strength increases exponentially with quartz cement (**Figure 7**). Dynamic elastic moduli and the P- and S- wave velocities from which they were calculated increase linearly with BGR alone; including the normalized grain contact length does not improve the fit (**Figure 8**).

It is important to note that all of the mechanical data are also well correlated to porosity. Tensile strength shows the poorest fit to porosity, with an R^2=0.79 compared to the 0.90 shown in **Figure 7**. These relationships reflect the interrelated nature of the micromorphologic parameters investigated, which is well expressed by the strong correlation between BGR and porosity shown in **Figure 3a**.

An implication of these results is that for quartz-cemented quartz arenites, increasing the number of grain-to-grain contacts stiffens the solid framework response to low strains, such as those imposed by ultrasonic elastic waves (**Figure 8**). Increasing contact length therefore does not have a substantial impact on elastic properties. It does, however, affect inelastic failure, as indicated by compressive strength data (**Figure 6**). Previous experimental and theoretical studies (Yin and Dvorkin, 1994; David et al. Dvorkin, Wong and Wu, 1995; Yang and Wong) suggest that increasing contact length through the addition of even small amounts of cement distributes loads at contacts. Increasing the number and length of contacts would reduce the stress per contact and distribute the total load. If the assumption is made that failure initiates at grain contacts, then the reduction in contact stress achieved by increasing the number and length of contacts would increase the total load the rock could withstand before failure in compression.

Indirect tensile strength measurements are inherently variable. Our data, however, show a strong trend suggesting that the contacts between quartz overgrowths are not purely frictional; i.e. bonds between quartz overgrowths impart an effective tensile strength to the material (**Figure 7**). These results suggest that for a given intergranular volume or packing arrangement, the sample with more quartz cement will have greater tensile strength. Sandstones in which grain mineralogy differs from cement mineralogy, and sands that lack cement, are expected to exhibit different behavior than what we have documented for these quartz-cemented quartz arenites.

Diagenetic Path and Mechanical Behavior

As indicated earlier, diagenesis in sandstones occurs in two distinct stages. Physical compaction dominates early diagenesis, but is arrested when grain contact cements become sufficiently well distributed to stiffen the grain framework and prevent further compaction. Therefore at early stages of diagenesis, BGR increases but contact length remains small, but after the initiation of cementation, contact length increases rapidly. The relationships presented suggest that early compaction and consolidation, which increase BGR, have the greatest impact on elastic properties, whereas compressive and tensile strength subsequently increase with quartz cementation. The effect of percent cement on tensile strength is particularly notable.

UW PILOT STUDIES

In addition to detailed study of the relationship between diagenetic path and both permeability and mechanical properties of the St. Peter Sandstone, our DOE grant provided limited support for two other studies. One of these is an investigation of the relationship between diagenesis and character of deformation bands in the St. Peter Sandstone. Both dilation and shear deformation bands are present in the study area, and shear bands record cataclasis in some locations and particulate flow in the absence of cataclasis in others. Our preliminary study is focused on understanding the timing of formation of these different types of deformation bands with respect to cementation, with the goal of relating deformation style to the rock characteristics documented above.

The second study has focused on degree of localization of fault-zone deformation in mudstone during progressive diagenesis (Cook et al., in prep.). This work addresses the space-time evolution of rocks in the damage zone of the San Gregorio fault, which is part of the San Andreas fault system in central California. We show that as the rocks become progressively

better consolidated and cemented, deformation becomes progressively more localized, such that foliation produced by particulate flow is overprinted by deformation bands, which are overprinted by discrete fractures and faults. Fluid flow through the latter fractures and faults is recorded by precipitation of calcite cement. Thus, the rocks record an evolution from permeability-reducing to permeability-enhancing deformation with progressive diagenesis.

UMass Modeling Study: Summary of Plourde et al. (in prep.)

Introduction

The mechanical and hydrologic behavior of clastic rocks and sediments is fundamentally controlled by variables such as grain size and shape, grain and cement mineralogy, and %cement - parameters that are not used directly in field-scale models of coupled flow and deformation. To improve our understanding of the relationship between these micromechanical properties and bulk behavior we present the use of a combination of discrete element method (DEM) and poroelastic models parameterized by data from natural samples to isolate and compare the influence of changes in the mechanical and hydrologic properties of granular porous media due to changes in a key variable, the degree of cementation. We address the role of changes in cementation by using meso-scale, two dimensional DEM models. The changes in hydrologic properties are evaluated using a correlation factor between the DEM models and natural samples. By correlating the amount of cementation in the DEM models and natural samples we can evaluate the effects of changes in cementation on both the mechanical and hydrologic properties of clastic media. The focus of this research is on the relative importance of cementation on hydro-mechanical behavior of sedimentary rocks, which has implications for both aquifer/ reservoir characterization and geologic carbon sequestration research and development.

We focus on isolating the role of cementation on the evolution of the hydrologic and mechanical behavior of siliciclastic sediments dominated by strong detrital grains, such as quartz. We specifically seek to evaluate the influence of progressive cementation on elastic properties of those materials, as well as the coupled evolution of porosity and permeability. These properties are then used to evaluate the large scale behavior of coupled hydrologic and mechanical transients in field scale problems. We begin by discussing the development, execution, and results from DEM-based simulations with variable cementation. We then discuss correlations to natural samples to complete the data set, and finally discuss the parameterization of continuum scale poroelastic models and present results evaluating the relative role of mechanical versus hydrologic properties in controlling key system behavior.

Coupled mechanical and hydrologic behavior

Coupled processes in geology commonly involve strongly nonlinear relationships among state variables (e.g., fluid pressure and stress state) and their associated dependencies on rock properties. For example, the fluid permeability in a porous medium relates fluid flux and fluid pressure through Darcy's law where the permeability can be a function of effective stress. The coupling between hydrologic and mechanical processes can be examined in two arbitrary ways: 1) the effect of fluid pressure on the mechanical response (effective stress) and 2) the effects of mechanics (strain and stress) on the hydrologic response, especially via permeability

modification. These coupling pathways can be equally important. However, either one or both are often ignored; many conditions or situations call for simplification in the form of neglecting one 'direction' of this coupling. For example, one of the assumptions in the development of the transient groundwater flow equation is that deformations are small and reversible (i.e., elastic deformation), and permeability remains unaltered. Numerical models and analytical solutions can aid in the analysis of the importance of the competing hydromechanical effects.

The poroelastic response of aquifers has been investigated in a number of different contexts. In fact, the well-known hydrogeologic concept of specific storage is a poroelastic process (Green and Wang, 1990) that describes the volume change of water and aquifer material due to a hydraulic head change under a set of specific assumptions. Assumptions of vertical strain and constant total stress allow one to derive the familiar hydrogeologic storage coefficient. Aside from material properties, during the withdrawal of water from a well it is well known that deformation occurs not only in the vertical dimension but also in horizontal directions (Burbey, 1999; Burbey, 2001; Narasimham, 2006). Numerous studies have presented the influence of relaxing the classic vertical strain assumptions to predict complete 3-dimensional poroelastic behavior of aquifers (Helm, 1994; Burbey et al., 2006; Burbey, 2006).

The effects of cement on the mechanical behavior of rock

The amount and type of cement located at grain contacts substantially impacts the elastic behavior of the grain-cement system. The effective elastic properties of a random packing of identical spherical particles was expressed through its porosity, coordination number (average number of contacts per sphere), the radius of the particle, and the normal and tangential stiffness of a two sphere combination (Digby, 1981; Winkler, 1983). Dvorkin et al. (1991) examined the normal interaction of two spherical elastic grains separated by an elastic layer of cement. The distribution of stresses was found to be a function of the ratio of the stiffness of the cement to the stiffness of the particle. The solutions also show that the amount of cement influences the effective elastic properties. Additionally, the hydrogeologic storage capacity of a porous medium is also influenced by changes in cement, as the fundamental micromechanical processes that give rise to this macroscopic phenomenon are dependent on the mechanical properties of the material.

The effects of cement on hydrologic behavior of rock

Cementation also influences the hydrologic properties of clastic media, namely permeability and porosity, by reducing the connectivity and size of pore throats between grains and reducing the total pore volume of the granular skeleton. Permeability is the key factor controlling the productivity of aquifers and reservoirs and is therefore well documented in geologic literature (Kozeny, 1927; Carmen, 1937; Carmen, 1956; Archie, 1950; Pape et al., 2000; Dutton et al., 2002; Olsen et al., 2008; Ehrenberg, 1990). Archie (1942) established a relationship between the amount of cement and the permeability of granular material using a cementation exponent. Archie's cementation factor is widely used in the development hydrocarbon and groundwater resources (Salem, 2001; Azar et al., 2008). The cementation factor in Archie's equation is a function of the number, size and shape of the pores and the shape of the grains. Ehrenberg (1990) suggests that permeability is largely a function of intergranular macroporosity, which is largely controlled by the diagenetic processes of compaction and cementation. Changes in permeability

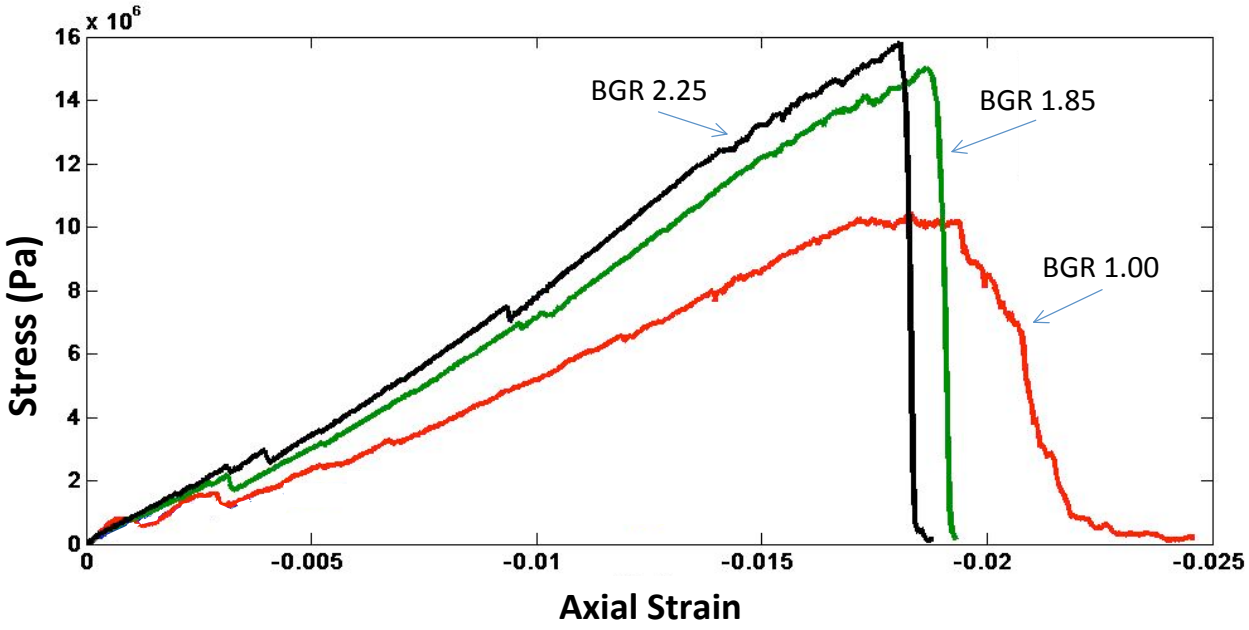

Figure 1 Stress-strain plots for each BGR in the DEM models

resulting from changes in porosity in clastic rocks are often evaluated using the Kozeny-Carman equation. The grain-bridging cements that have the greatest impact on mechanical properties also produce the greatest permeability reduction, as compared to pore lining or pore-filling cements.

DEM Modeling

In the work summarized here, we focused on simulating the addition of cementing material to grains by bonding individual discrete elements each other. Since the bonds are modeled as point to point (line) constraints, the bond thickness is undefined and we cannot use an area calculation to quantify the amount of cementation in the models. Therefore, a quantity to characterize the relative number of bonds in each model is needed. The bond-to-grain ratio (BGR) defined earlier as the number of bonds in the model divided by the total number of grains (particles) is such a quantity. This is similar to the concept of a coordination number but instead of quantifying the number of contacts it refers to the average number of bonded (or cemented) contacts per grain. The BGR can be used both to quantify the amount of simulated cement in the models and to compare the models to the natural samples we have studied.

The 2D DEM models are designed to replicate laboratory triaxial tests (Boutt and McPherson, 2001). Triaxial tests are generally performed on natural rock cores in order to determine the elastic mechanical properties (e.g. Young's modulus and Poissons' ratio) of the samples. The same objective can be accomplished with 2D biaxial tests to evaluate the mechanical properties of differently cemented (i.e. models with different BGR) discrete element assemblies.

Table 1: The elastic and inelastic results for the ellipsoidal grain simulation as a function of BGR. Percent cementation increases with higher BGRs.

BGR	Young's Modulus (Pa)	Poisson's Ratio	Shear Modulus (Pa)	Yield Strength (Pa)
0.5	2.6×10^8	0.56	8.9×10^7	2.1×10^6
1.00	6.9×10^8	0.48	2.4×10^8	1.0×10^7
1.85	9.3×10^8	0.28	3.6×10^8	1.5×10^7
2.25	1.2×10^9	0.27	4.8×10^8	1.6×10^7

In order to evaluate the mechanical properties of the models, we loaded the discrete element assemblies until failure, defined as the first major loss in strength in a plot of axial stress versus axial strain (relative to the long axis of the assembly). In numerical and laboratory tests, inelastic deformation is expressed as non-linearities on these axial stress-strain curves. The change in slope indicates grain re-arrangement via frictional sliding and/or bond breakage. By calculating the slope of the linear portion of the axial stress-strain curves for each simulation, we estimated the Young's modulus as function of the amount of cementation in each model. DEM models were parameterized with the goal of isolating the role of variable amounts of cement on the resulting bulk material parameters. Important parameters in DEM models include the stiffness and breaking strength of bonds, grain-contact normal and shear stiffness, and intergranular friction.

We designed three models with BGR's of 1.00, 1.85, and 2.25, respectively, which capture the range of BGRs observed in natural samples (1.4-2.24; UW Figure 3a). A BGR of 1.00 represents the lowest value of cement that could still be considered a lithified material. Below this value, the material properties are those of uncemented sand. In the models, a BGR of 2.25 represents the highest end member corresponding to the case where additional cementation provides no stiffening or strengthening. The slope of the stress-strain curve for each cementation simulation provides a value of Young's Modulus for that model (Figure 1). At a value of BGR=1.00, the slope of the stress-strain curve is relatively flat and likely represents a weakly cemented sand. Post-peak stress, the cirve does not drop steeply, but reflects additional post-yield strength. At larger values of BGR, the materials stiffen dramatically and exhibit post-yield behavior indicative of brittle materials. For a BGR of 1.85 the slope of the stress-strain curve is much steeper than that of BGR 1.00. The effect of additional cementation from BGR 1.85 to 2.25 yields little change in mechanical behavior resulting in a modest increase in Young's modulus and yield strength. Increasing values of Young's modulus from BGR 1.00 to BGR 2.25 indicate the model stiffens with increased cementation.

Contrastingly, as Young's Modulus increases, Poisson's ratio decreases because the stiffening of the granular skeleton resists deformation from changes in stress. In order to simplify reporting of results, the changes in the elastic response have been calculated as a change in shear modulus.

The shear modulus is calculated for each BGR. The shear modulus shows a 1.4-fold increase in from a BGR of 1.00 to a BGR of 2.25 (Table 1). The response of the shear modulus to

Table 2: Input parameters utilized in Poroelastic simulations. Mechanical properties are from DEM simulations while hydraulic properties are from laboratory data.

BGR	Altered Properties	Shear Modulus (Pa)	Permeability (m^2)	Porosity (%)
1.00				
	Mechanical	$7x10^8$	$1x10^{-13}$	15
	Hydrologic	$9x10^8$	$1x10^{-12}$	25
	Mech. & Hydro.	$7x10^8$	$1x10^{-12}$	25
1.85				
	Mechanical	$9x10^8$	$1x10^{-13}$	15
	Hydrologic	$9x10^8$	$3x10^{-14}$	12
	Mech. & Hydro.	$9x10^8$	$3.x10^{-14}$	12
2.25				
	Mechanical	$1x10^9$	$1x10^{-13}$	15
	Hydrologic	$9x10^8$	$9x10^{-15}$	8
	Mech. & Hydro.	$1x10^9$	$9x10^{-15}$	8

changes in cement content as quantified by the BGR shows two interesting trends. First, the magnitude of change is small considering the change in BGR from an almost un-cemented to a fully cemented state. Second, the increase in shear modulus with BGR does not follow the linear trend suggested by the laboratory data collected by the UW group (UW Figures 6 and 8). Instead, the stiffening affect of adding cement decreases at higher cement (higher BGR) levels. Additional modeling shows that changes in elastic behavior are insignificant (less than 1%) in DEM models at BGR's larger than 2.25. This suggests a threshold limit to the effect of cement on the mechanical behavior of sandstones, where further increases in cement content do not affect mechanical behavior.

Poroelastic Modeling

Two dimensional, axially symmetric, poroelastic models are used to investigate the effects of micro-scale mechanical and hydrologic properties on aquifer-scale fluid flow and deformation. This research utilizes Comsol Multiphysics, a finite element method code in which subroutines solve the equations of linear poroelasticity and provide transient fluid-solid deformation solutions. These equations are solved under assumptions of axi-symmetry using Lagrange triangular finite elements. The conceptual model and model domain for the poroelastic models is a cylindrical confined aquifer/reservoir that is 100 meters thick and its boundaries extend 160 kilometers in radial distance. The initial hydraulic head throughout the entire domain is specified at a value of 200 meters. A fully penetrating pumping well lowers the hydraulic head a constant value of 150 meters. The boundary condition of specified head was chosen in lieu of a specified flux (i.e. pumping rate) to explore the transients that develop in models with drastically different hydraulic conductivities. This approach enables the observation of the progression of dewatering and deformation induced from the pumping well across the aquifer as a result of the

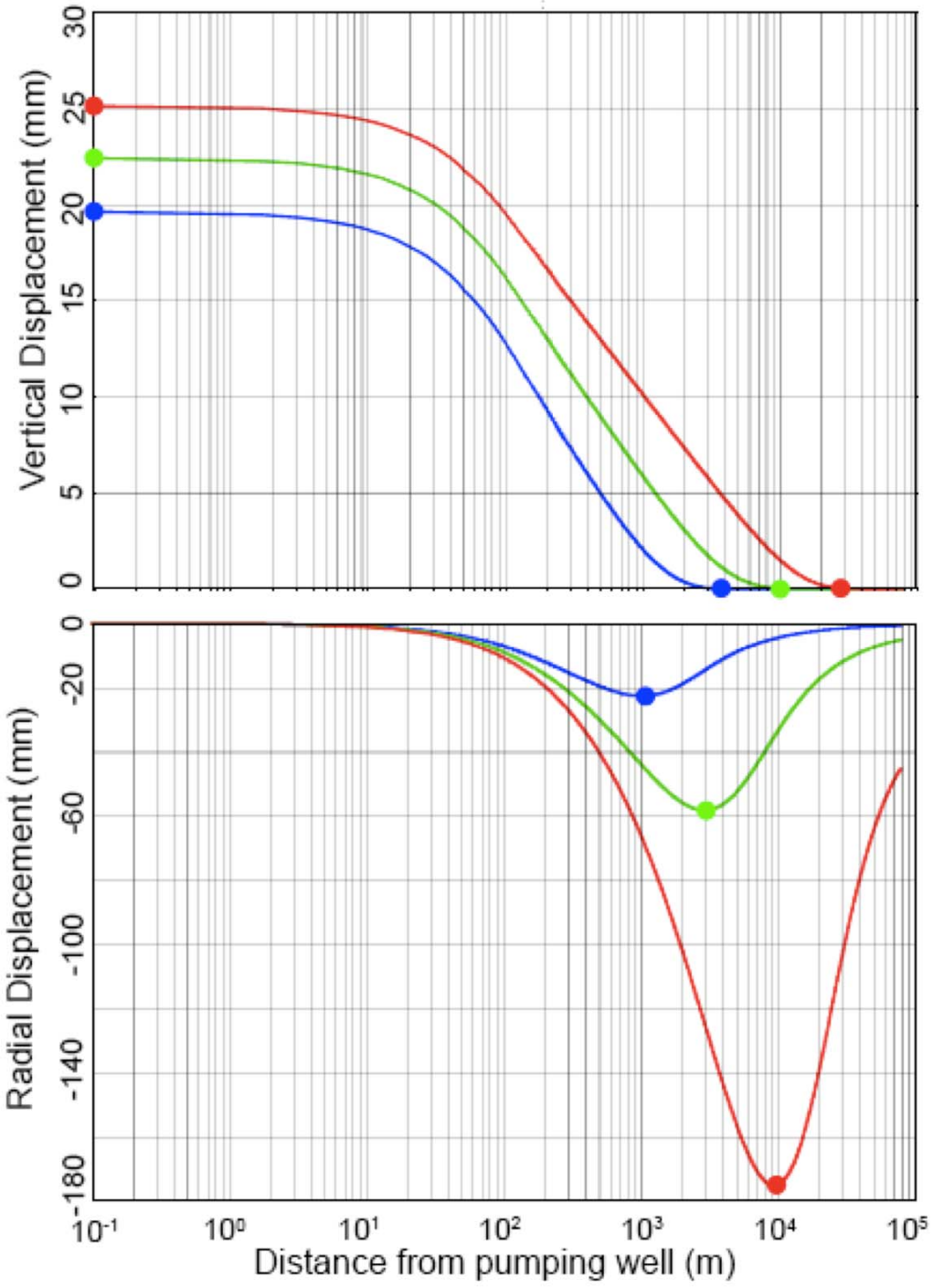

Figure 2: Plots of the magnitude and distance of surface deformation as a function of the distance from the pumped well. a) Vertical and b) radial deformation from a poroelastic model showing the points plotted in Figure 4.

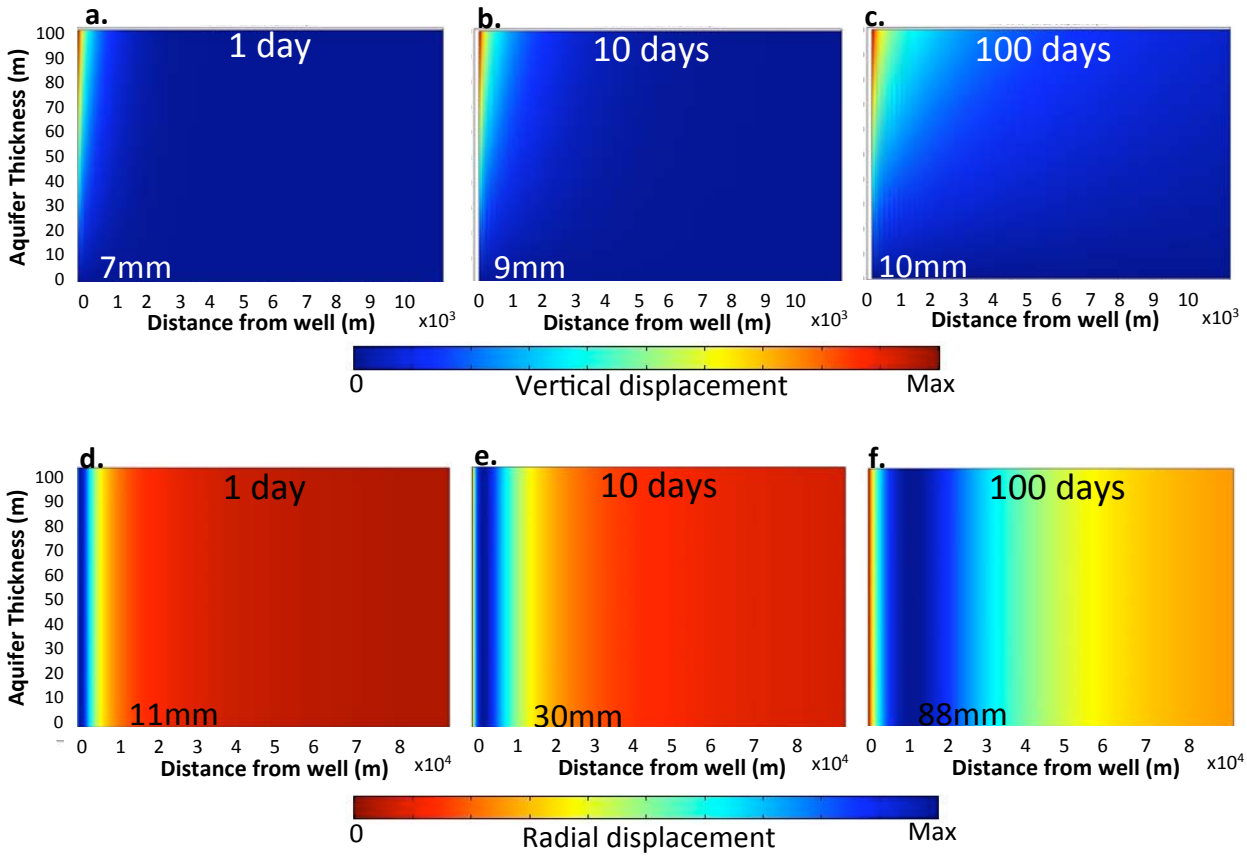

Figure 3: Contour plots of vertical and radial deformation near the pumping well after a and d) 1, b and e) 10 and c and f) 100 days of pumping, respectively. The snapshots of vertical displacement are zoomed into the region near the pumped well (the pumped well is on the left) to show the entire thickness of the aquifer but only extend 10 km horizontally. The snapshots of radial displacement are the set up the same as the vertical displacement except they extend 80 km horizontally.

changes in properties. The remaining hydraulic boundary conditions are zero flux (or no flow / impermeable boundaries). For the mechanical boundary conditions, the boundary condition at the well is zero radial displacement and zero vertical stress. The other boundaries are allowed to displace in the radial and vertical directions, except the bottom boundary, which is fixed to have zero vertical displacement.

Model Parameterization

The constitutive behaviors from the DEM models are used to calculate elastic mechanical properties (shear moduli) as a function of percent cement and used as input parameters for the poroelastic models. Three sets of poroelastic models (nine models in total) are used to evaluate the influence of elastic mechanical (shear modulus) and hydrologic (porosity and permeability) properties on fluid flow and deformation in the aquifer. Using BGR as a parameter to interrelate DEM properties and properties from the laboratory measurements of St. Peter Sandstone we assigned shear moduli, porosity, and hydraulic conductivity for a specific value of BGR.

The first set of models investigated the influence of changing shear modulus on fluid flow and deformation while holding hydrologic properties constant. One model was run for each BGR, with the corresponding value of shear modulus (Table 2). The second set of simulations evaluated the importance of only the hydrologic properties specific to each BGR (Table 2). These three models used identical mechanical properties but the hydrologic properties were assigned based on laboratory-derived hydraulic conductivity for each BGR. The third set of models incorporated the specific values of both the mechanical and hydrologic properties for each BGR. This model series allows us to specifically investigate the role of cementation in the hydrologic, mechanical, and hydromechanical response of a granular porous medium.

Poroelastic Modeling Results

For each simulation, the time evolution of displacements, stress, and hydraulic head (i.e. fluid pressure) was tracked. For the purpose of this analysis these components were examined at 1, 10 and 100 days after pumping was initiated. The magnitude of vertical and radial displacement as a function of distance from the pumped well (e.g. Figure 2) was analyzed at these times in each simulation. Figure 2a shows that the vertical displacement of an aquifer is greatest near the well and gently decreases in magnitude away from the well. This trend is similar at 1, 10, and 100 days with the exception that the area undergoing vertical deformation increased over time due to the growing influence of the cone of depression around the well. Figure 2b depicts the radial displacement of the aquifer as a function of distance away from the pumping well. One day after pumping starts, the magnitude of radial displacement (negative values indicated shortening of the aquifer in a radial sense) is small and localized in a zone 1000 m away from the pumping well, coincident with the point at which the vertical displacement becomes increasingly small. As time increase from 1 to 100 days the zone of radial deformation dramatically increases in magnitude and its maximum becomes further away from the pumping well.

Figure 3 depicts a series of filled contour plots of the aquifer for vertical (Figure 3 a, b and c) and radial deformation (Figure 3d, e and f) at 1, 10 and 100 days for the BGR 1.00 simulation with changes in the mechanical and hydrologic properties. To aid the comparison between the suite of 9 models being investigated, points on the x and y-axis at 1,10, and 100 days in Figure 2 are chosen for the magnitudes of maximum deformation and the distances from the pumped well at which the vertical deformation is zero and the horizontal deformation is a maximum.

Figure 4 presents a composite of the locations of the minimum and maximum displacements and magnitudes of deformation for the vertical and radial deformation in the simulations. All models show an increase in deformation and drawdown over the course of the 100 day simulations, with the greatest increases in the models with the lowest BGRs. The decrease in deformation with increasing BGR (percent cement) reflects the stiffening response of the granular porous medium with increasing cement observed in the DEM models. The magnitude and area of deformation vary with the mechanical and hydrologic properties of specific models.

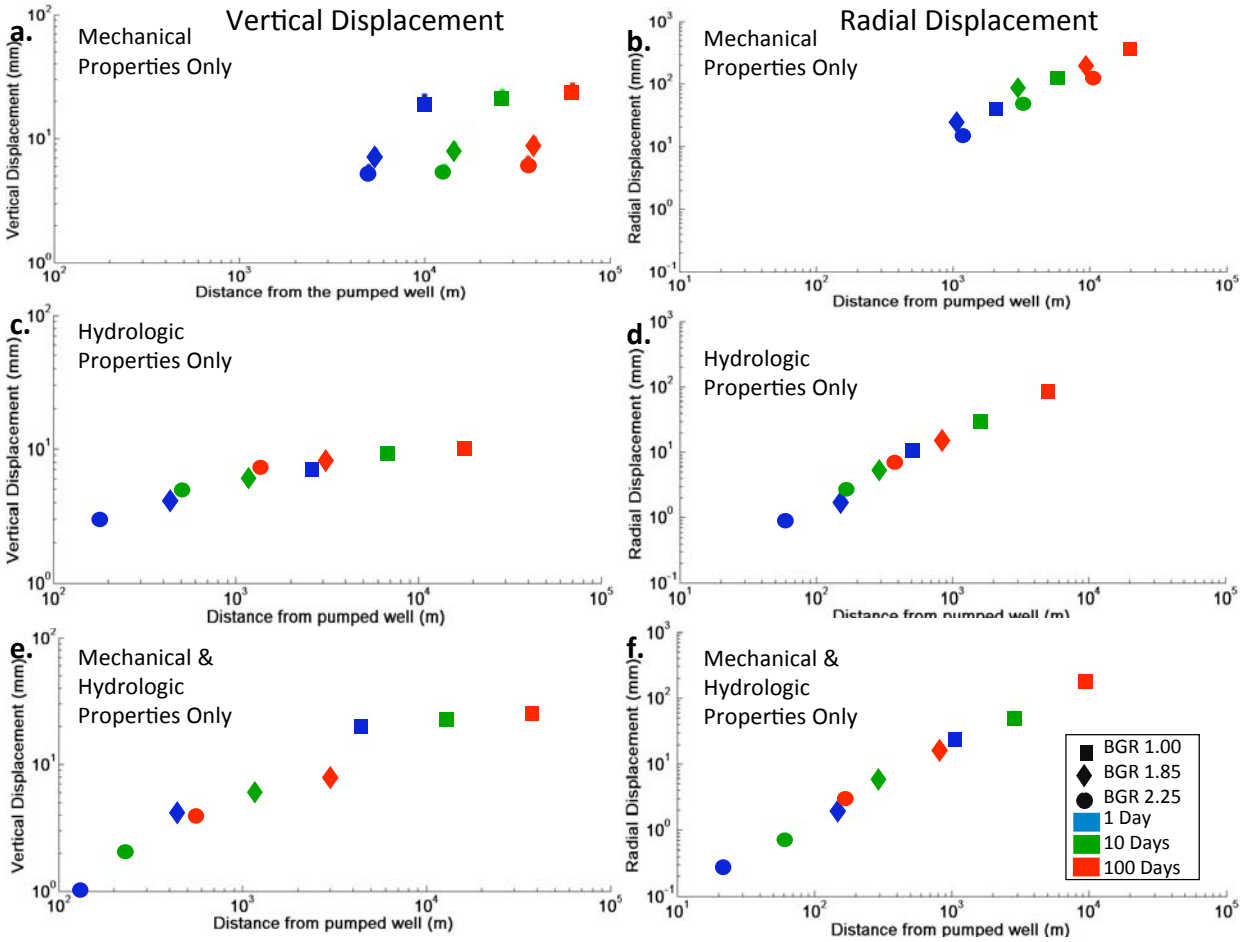

Figure 4: Vertical and radial deformation from the nine poroelastic models after 1, 10 and 100 days of pumping. a) Vertical displacement as a result of changing the shear modulus. b) Radial displacement as a result from only changing the mechanical properties. c) Vertical displacement as a result of changing only the hydraulic conductivity. d) Radial displacement results from changing only the hydrologic properties. e) Vertical displacement as a result of changing the shear modulus and hydrologic properties. f) Radial displacement results from changing the mechanical and hydrologic properties. Note the axis changes from the vertical to radial deformation plots.

In the first set of models, the shear modulus was changed for each simulation (Figure 4a and b). Although the magnitude of deformation for each model varies somewhat, the range of values is less than that of the models that included variations in hydrologic properties (Figure 4c, d, e and f). The comparison of Figure 4a and b to Figure 4c and d, e and f suggests that the hydrologic properties significantly control the magnitude and location of deformation. In the first set of models where only the shear modulus changes with BGR, the hydrologic properties are set to a maximum to isolate the effects of changes in shear modulus by allowing deformation to occur in a large portion of the aquifer (Table 2). The second set of models, where only the hydrologic properties are changed with each BGR, the models produce a wider range of magnitudes and show larger areas influenced by deformation compared to the first set of models.

The differences in the magnitude and timing of deformation suggest that poroelastic deformation is more sensitive to the changes in hydrologic properties than mechanical properties. The third set of models include both the mechanical and hydrologic influences of changes in cement. Varying both the mechanical and hydrologic properties resulted in slightly higher values of vertical and radial deformation for BGR 1.00 but lower values for BGR 2.25. For the most realistic case of including the changes in mechanical and hydrologic properties associated with changes in cementation, the decrease in BGR from 2.25 to 1.00 resulted in a 1.4- and 11.0-fold increase in vertical and radial deformation, respectively.

Conclusions

This meso-scale investigation revealed a direct correlation between micro-scale BGR and the mechanical response of a simulated granular porous medium. The BGRs are effective for correlating the amount of cement in the DEM models with natural samples as well as correlating the effects of changes in the amount of cementation with changes in permeability.

At the macro-scale, changes in mechanical and hydrologic properties directly influence the magnitude and area of aquifer deformation. The significant difference in sensitivity of the system to the mechanical properties alone versus its sensitivity to coupled mechanical and hydrologic properties demonstrates the importance of including hydrologic properties that are adjusted for changes in cementation in fluid storage and deformation studies. The large magnitude of radial deformation compared to vertical deformation emphasizes the importance of considering three dimensional deformation in fluid flow and deformation studies.

Related Work

This grant also provided funding for research that contributed to two publications focused on the relationship between hydrologic and mechanical properties and deformation behavior in uncemented and cemented porous media. Boutt et al. (2009) investigated the effect of hydrologic properties on the initiation and propagation of natural hydraulic fractures using coupled discrete element and lattice-Boltmann models of deformation and fluid flow. Model simulations were designed to replicate conditions of laboratory experiments where hydraulic fractures are generated. Models are to a first order consistent with the laboratory experiments and predict a strong dependence of deformation on the hydraulic diffusivity of the rock-fluid system. Hydraulic properties appear to influence the inelastic mechanical response of rock to fluid pressure transients.

Boutt (2010) explored the relationship between field-scale composite hydrologic properties and response to an applied surface load. The juxtaposition of fine-grained, low permeability units and high permeability deposits create a unique poro-mechanical response observed in a multi-level piezometer nest. This phenomenon is further investigated using coupled poroelastic modeling to quantify the extent of the aquifer impacted by the surface load. The dynamic load, produced by upstream dam releases of water, induces a measurable and extensive zone of deformation in the aquifer that is solely dependent on the stratigraphy of the site.

REFERENCES CITED (* mark papers supported by this grant)

Archie, G. (1942), The electrical resistivity log as aid in determining some reservoir characteristics, Trans. AIME, 146, 54-62.

Archie, G. (1950), Introduction to petrophysics of reservoir rock, AAPG Bulletin, 34, 943-961.

Azar, J., M. Javaherlan, and M. Pishvaie (2008), An approach to defining tortuosity and cementation factor in carbonate reservoir rocks, Journal of Petroleum Science and Engineering, 60 (2), 125{131.

Ahmed, U., S. Crary, and G. Coates (1991), Permeability estimation: the various sources and their interrelationship, Journal of Petroleum Technology, 43, 578-87.

Berg, R., (1970), Method of determining permeability from reservoir rock properties, Gulf Coast Association of Geologic Society Transaction 20, 303-17.

Bloch, S. (1991), Empirical prediction of porosity and permeability in sandstones, AAPG Bulletin, 75, 1145-1160.

* Boutt, D.F., Poroelastic loading of an aquifer due to upstream dam releases, Ground Water, doi: 10.1111/j.1745-6584.2009.00663.x, 2010.

Boutt, D. F., B. K. Cook, B. J. O. L. McPherson, and J. R. Williams (2007), Direct simulation of fluid-solid mechanics in porous media using the discrete element and lattice-Boltzmann methods, J. Geophys. Res., 112, B10209, doi:10.1029/2004JB003213.

* Boutt, D.F., L. Goodwin, and B. McPherson, The role of permeability and storage in the initiation and propagation of natural hydraulic fractures, Water Resources Research, 45 (W00C13), doi: 10.1029/2007WR006,557, 2009.

Boutt, D. F., and B. J. O. L. McPherson (2002), Simulation of sedimentary rock deformation: Lab-scale model calibration and parameterization, Geophys. Res. Lett., 29(4), 1054, doi:10.1029/2001 GL013987.

Burbey, T.J. (1999), Effects of horizontal strain in estimating specific storage and compaction in confined and leaky aquifer systems, Hydrogeology Journal, 7 (6): 521-532.

Burbey, T.J. (2001), Storage coefficient revisited: Is purely vertical strain a good assumption?, Ground Water, 39 (3): 458-464.

Burbey T.J. (2006), Three-dimensional deformation and strain induced by municipal pumping, Part 2: Numerical analysis. Journal of Hydrology, 330, 3-4, 422-434.

Burbey T.J, S.M. Warner, G. Blewitt, J.W. Bell, and E. Hill (2006), Three-dimensional deformation and strain induced by municipal pumping, part 1: Analysis of field data, Journal of Hydrology, 319 : 123 DOI 10.1016/j.jhydrol.2005.06.028.

Carman, P. C. (1937), Fluid flow through granular beds, Trans. Inst. Chem. Eng. London 15 150.

Carman, P. C. (1948), Some physical aspects of water flow in porous media, discuss. Faraday Soc. 3, 78.

Carman, P. C. (1956), The flow of gases through porous media. New York: Academic Press.

* Cook, J.E., L.B. Goodwin, and D.F. Boutt, Systematic diagenetic changes in the grain-scale morphology and permeability of a quartz-cemented quartz arenite. AAPG Bulletin, in review.

* Cook, J.E., L.B. Goodwin, and D.F. Boutt, Systematic diagenetic changes in the mechanical properties of a quartz-cemented quartz arenite. In prep.: to be submitted to Journal of Geophysical Research.

* Cook, J.E. and L.B. Goodwin Spatial and temporal evolution of fault zone structures in sediment: An example from the San Gregorio fault, California. In prep.: to be submitted to Lithosphere.

Comsol multiphysics modeling guide. Comsol AB, 1994-2006.

David, C, B. Menendez, and Y. Bernabe (1998), The mechanical behavior of synthetic sandstone with varying brittle cement content: International Journal of Rock Mechanics and Mining Sciences and Geomechanics Abstracts, 35: 759-770

Digby, P.J., The effective elastic moduli of porous granular rock, J. Appl. Mech., 48(4), 803–808, 1981.

Dillon, C. G., R. H. Worden, and S.A. Barclay (2004), Simulations of the effects of diagenesis on the evolution of sandstone porosity: Journal of Sedimentary Research, 74: 877-888.

Dunn, D. E., L. J. LaFountain, and R.E. Jackson (1973), Porosity dependence and mechanism of brittle fracture in sandstones: Journal of Geophysical Research, 78: 2403-2417.

Dutton, S., C. White, B. Willis, and D. Novakovic (2002), Calcite cement distribution and its effect on fluid flow in a deltaic sandstone, frontier formation, Wyoming source, AAPG Bulletin, 86.
Dvorkin, J., G. Mavko, and A. Nur, (1991), The effect of cementation on the elastic properties of granular materials, Mechanics of Materials, 12: 207–217.
Dvorkin, J., A. Nur, and H. Yin (1994), Effective properties of cemented granular materials: Mechanics of Materials, 18: 351 – 366.
Ehrenberg, S. (1990), Relationship between diagenesis and reservoir quality in sandstones of Garn formation, Haltenbanken, mid-Norwegian continental shelf, AAPG Bulletin, 74 (10), 1538-1558.
Gal, D., Dvorkin, J., and A. Nur (1998), A physical model for porosity reduction in sandstones: Geophysics, 63: 454-459, doi: 10.1190/1.1444346.
Green, D., and H. Wang (1990), Specific storage as a poroelastic coefficient, Water Resour. Res,. 26, 1631-1637.
Hashin, Z., and S. Shtrikman (1963), A variational approach to the elastic behavior of multiphase materials: Journal of the Mechanics of Physical Solids, 11: 127-140.
Helm, Donald, C. (1994), Horizontal aquifer movement in a Theis-Thiem confined system, Water Resour. Res,. 30, 953-964.
Kelly, J. L., B. Fu, N. T. Kita, and J. W. Valley (2007), Optically continuous silcrete quartz cements of the St. Peter Sandstone; high precision oxygen isotope analysis by ion microprobe: Geochimica Et Cosmochimica Acta, 71: 3812-3832, doi: 10.1016/j.gca.2007.05.014.
Kozeny, J. (1927), Über die kapillare Leitung des Wassers im Boden (Aufstieg, Versickerung und Anwendung auf die Bewässerung), Sitz. Ber. Akad. Wiss. Wien. Math. Nat. (Abt. IIa) 136a, 271-306.
Lundegard, P. D. (1992), Sandstone porosity loss; a "big picture" view of the importance of compaction: Journal of Sedimentary Petrology, 62: 250-260.
Narasimhan, TN (2006), On storage coefficient and vertical strain, Ground Water, 44 (3): 488-491.
Mai, H and R. H. Dott (1985), A subsurface study of the St. Peter Sandstone in southern and eastern Wisconsin: United States (USA), University of Wisconsin-Extension, Geological and Natural History Survey, Madison, WI, United States (USA), Information Circular 47, 26 p.
Mavko, G., T. Mukerji, and J. Dvorkin (2009), The Rock Physics Handbook, New York, Cambridge University Press, 511 p.
McBride, E. F. (1989), Quartz cement in sandstones; a review: Earth-Science Reviews, 26: 69-112.
Mowers, T. T., and Budd, D. A. (1996), Quantification of porosity and permeability reduction due to calcite cementation using computer-assisted petrographic image analysis techniques: AAPG Bulletin, 80: 309-322, doi: 10.1306/64ED87C8-1724-11D7-8645000102C1865D.
Odom, I. E., T. N Willand, and R. J. Lassin (1979), Paragenesis of diagenetic minerals in the St. Peter Sandstone (Ordovician), Wisconsin and Illinois, *in* P. A. Scholle and P. R. Schluger, eds., Aspects of diagenesis: SEPM Special Publication 26: 425-443.
Olsen, C., T. Hongdul, and I. Fabricius (2008), Prediction of archie's cementation factor from porosity and permeability through speci_c surface, Geophysics, 73 (2), E81-E87.
Panda, M. N., and L. W. Lake (1995), A physical model of cementation and its effects on single-phase permeability: AAPG Bulletin, 79: 431-443, doi: 10.1306/8D2B1552-171E-11D7-8645000102C1865D.
Pape, H., C. Clauser and J. Iffland (2000). Variation of permeability with porosity in sandstone diagenesis interpreted with a fractal pore space model, Pure appl. Geophys., 157, 603-619.
* Plourde, K., D.F. Boutt, L.B. Goodwin, and J. Cook, Quantifying the effects of cementation on hydromechanical properties of granular porous media using discrete element models, In prep.: to be submitted to Water Resources Research.
Reuss, A. (1929), Berechnung der fliessgrenzen von mischkristallen auf grund der plastizitatsbedingung fur einkristalle: Z. Ang. Math. Mech., 9: 49 – 58.
Salem, H. (2001), Determination of porosity, formation resistivity factor, archie cementation factor, and pore geometry factor for a glacial aquifer, Energy Sources, 23 (6), 589-596.
Scholle, P. A. (1979), A Color Illustrated Guide to Constituents, Textures, Cements, an Porosities of Sandstones and Associated Rocks, The American Association of Petroleum Geologists Memoir 28: 201 p.

Storvoll, V., and K. Bjorlykke (2004), Sonic velocity and grain contact properties in reservoir sandstones: Petroleum Geoscience, 10: 215-226, doi: 10.1144/1354-079303-598.
Winkler, K.W., (1983), Contact stiffness in granular porous materials: comparison between theory and experiment, Geophysical Research Letters, 10: 1073-1076.
Wong, T.-f., and L-C. Wu (1995), Tensile stress concentration and compressive failure in cemented granular material: Geophysical Research Letters, 22: 1649-1652.
Worden, R. H., and Morad, S. (2000), Quartz cementation in oil field sandstones; a review of the key controversies, *in* R.H. Worden and S. Morad, eds., Quartz cementation in sandstones: Special Publication of the International Association of Sedimentologists 29: 1-20.
Yin, H., and J. Dvorkin (1994), Strength of cemented grains: Geophysical Research Letters, 21: 903-906, doi: 10.1029/93GL03535.
Zang, A., and T-f. Wong (1995), Elastic stiffness and stress concentration in cemented granular material: International Journal of Rock Mechanics and Mining Sciences and Geomechanics Abstracts, 32: 563-574.